

Green Chemistry

Accepted Manuscript



This is an *Accepted Manuscript*, which has been through the Royal Society of Chemistry peer review process and has been accepted for publication.

Accepted Manuscripts are published online shortly after acceptance, before technical editing, formatting and proof reading. Using this free service, authors can make their results available to the community, in citable form, before we publish the edited article. We will replace this *Accepted Manuscript* with the edited and formatted *Advance Article* as soon as it is available.

You can find more information about *Accepted Manuscripts* in the [Information for Authors](#).

Please note that technical editing may introduce minor changes to the text and/or graphics, which may alter content. The journal's standard [Terms & Conditions](#) and the [Ethical guidelines](#) still apply. In no event shall the Royal Society of Chemistry be held responsible for any errors or omissions in this *Accepted Manuscript* or any consequences arising from the use of any information it contains.

Synthesis and Characterization of an Extractive-based Bio-Epoxy Resin from Beetle Infested *Pinus contorta* Bark

Pei-Yu Kuo¹, Mohini Sain^{1, 2, 3} and Ning Yan^{1, 2,*}

¹ Faculty of Forestry, University of Toronto, 33 Willcocks Street, Toronto, ON, Canada, M5S 3B3

² Department of Chemical Engineering and Applied Chemistry, University of Toronto, 200 College Street, Toronto, ON, Canada, M5S 3E5

³ Department of Chemical Engineering and Applied Chemistry, King Abdullah University of Science & Technology, Thuwal 23955-6900, Kingdom of Saudi Arabia

*Corresponding author: (NY) Tel.: +1(416)946-8070, E-mail: ning.yan@utoronto.ca

This work outlines the synthesis and characterization of a green epoxy resin derived from bark extractives. The resins were prepared at various temperatures and catalyst amounts to determine an optimal for the yield and epoxy equivalent weight value. FTIR and NMR techniques were used to characterize the chemical structures of extractive-based epoxy (E-epoxy) monomers. Measurement results indicated a successful epoxidation of bark extractives after reaction with epichlorohydrin. GPC results revealed that the molecular weights and polydispersities of E-epoxy monomers were lower than that of lignin epoxy (L-Epoxy) monomers. The curing kinetic parameters calculated with the Kissinger method and the Model-Free method showed that E-Epoxy had a lower curing activation energy value than petroleum-based epoxy (P-Epoxy). Compared to P-Epoxy, E-Epoxy displayed comparable tensile strength and thermal stability. Research outcome demonstrated promises of using bark extractives to synthesize epoxy resins replacing toxic bisphenol A.

1. Introduction

Epoxy resins have widespread uses ranging from sealing integrated circuits to rocket coatings due to their high strength, good compatibility with most materials, and great thermal stability. However, with the recent awareness of toxicity associated with a bisphenol A (BPA), a key ingredient of epoxy resin, there is a need to develop alternative safe raw materials for the resin synthesis. During the past decade, researchers have explored several natural resources to replace BPA, such as vegetable oil (soybean oil¹⁻², linseed oil³, palm oil⁴, castor oil⁵ and cashew nut shell liquid⁶), simple polyols⁷, lignin⁸⁻⁹, rosin¹⁰, and liquefied biomass¹¹⁻¹³. These polymers can reduce dependency of the resin synthesis on petroleum resources and have the potential to be also biodegradable. Among these alternatives, vegetable oil, liquefied biomass, and lignin have emerged as the most promising materials, mainly owing to their commercial feasibility¹⁴. Nevertheless, these renewable resource-derived polymers have limitations. For example, the aliphatic structure of epoxidized oil results in low mechanical strength and poor thermal stability¹⁵. In order to improve these properties, liquefied biomass, with a high aromatic ring structure content, is used to enhance polymer mechanical and thermal performance¹⁶. However, the liquefaction process is energy intensive and requires toxic solvents, like phenol¹⁷. Lignin, the major waste material from the pulping industry, has been used to produce lignin-based epoxy with good mechanical performance and thermal stability. However, the molecular weight of lignin ranges from 2,000 Da to 50,000 Da¹⁸, leading to high viscosities that may cause difficulties during manufacturing or use since a major application of epoxy resins is in adhesives which require moderate viscosities in order to perfectly wet the substrate surfaces¹⁹. On the other hand, bark extractives contain large amounts of low molecular weight polyphenols and require less energy to extract. They have good potentials to be used as alternative materials to replace BPA. However, there is no reported work on bark extractive-based epoxy resin in the literature.

Tree bark, a waste material of timber processing, is abundant, renewable, and rich in phenolic compounds. Compared to wood, bark contains a higher amount of lignin and polyphenols (42-55%)²⁰. However, bark is usually considered to be a waste and is used as firelogs or burnt as hog fuels, despite having a heating value two times lower than fuel oil²¹. Recently, various polymers have been developed from bark, including novolac²² and resol-type²³ phenol formaldehyde resins (PF) as well as polyurethane²⁴. Low molecular weight polyphenolic compounds can be extracted from bark using various solvents, such as acetone, ethanol, methanol, organic solvent mixtures, and 1 % NaOH_(aq). Among these extraction, 1 % NaOH_(aq) was reported to be able to extract the phenolic compounds from barks with a high yield²⁵. Most importantly, the alkaline treatment has shown promise in achieving complete utilization of lignocelluloses without little impact to the environment²⁶. In addition, epoxy resins are synthesized with epichlorohydrin under alkali condition, and thus, the remaining sodium hydroxide in the bark extractives could also promote the epoxidation reaction. Although alkali treatment dissolves a large amount of low molecular weight polyphenols, other fractions of bark are also extracted that include lignin, cellulose, and hemicellulose. These components, which contain large amount of hydroxyl groups, can also react with epichlorohydrin. Thus, in this study, commercial lignin and cellulose were also included as model compounds to elucidate some of the characterization results of bark extractive based epoxy resins.

The objective of this study is to develop a novel type of epoxy monomers from bark extractives via a conventional epoxy resin synthesis process. The chemical structures of uncured monomers were investigated using Fourier transform infrared spectroscopy (FTIR) as well as nuclear magnetic resonance spectroscopy (NMR). Resin molecular weight and curing behaviour were studied

using gel permeation chromatography (GPC), and differential scanning calorimetry (DSC), respectively. Finally, thermal stability and mechanical performance of the cured bark-based resins were examined and compared to conventional BPA derived epoxy resins using thermogravimetric analysis (TGA) and a universal mechanical tester.

2 Materials and Methods

2.1 Materials

Mountain pine beetle infested lodgepole pine (*Pinus contorta*) bark was provided by FP-Innovations. Cellulose microcrystalline powder, epichlorohydrin (99%), dichloromethane, and tetrabutylammonium hydroxide solution (1.0 M in methanol) were purchased from Sigma Aldrich, ON, Canada. Sodium hydroxide (pellet), acetone (>99.5%) and 1,4-dioxane (99%) were purchased from Caledon Laboratory Chemicals, ON, Canada. Lignin, protobind 1000, was purchased from ATM India Ltd, Maharashtra, India. EPON 863 Epoxy resins and EPIKURE W amine type curing agent were supplied by Momentive Specialty Chemicals, OH, USA.

2.2 Methods

2.2.1 Bark Extraction

Bark extractives were obtained from bark chips using 1 % NaOH_(aq) solution at 90 °C for two hours with a 10:1 solvent/bark weight ratio. After filtering the residue fraction, the concentrated extractives were spray-dried using a laboratory spray drier (Yamato GB210) under the following conditions: inlet temperature of 160 °C, outlet temperature of 60 °C and air pressure of 0.1 MPa.

2.2.2 Synthesis of bark extractive epoxy resins

Extractive-based epoxy resins were prepared following a similar method as reported for commercially available resins. Bark extractives (15 g), epichlorohydrin (150 g), 1,4-dioxane (150g) and tetrabutylammonium hydroxide solution (2 mL) were placed into a round bottom 3-neck glass flask and the temperature was raised to 60 °C while stirring. An excess of epichlorohydrin was used in a mass ratio of bark extractives to epichlorohydrin of 1 to 10. The experiments were carried out following a two-factor design, including three synthesis temperatures (40°C, 60°C, 100 °C) and three catalyst molar ratios (0.5mol, 1mol, 2 mol). 50 % w/w sodium hydroxide_(aq) was then slowly added to the mixture using a pressure-equalizing dropping funnel while stirring. The flask was kept at 60 °C for a total of 6 hours to achieve the addition reaction of epichlorohydrin and the ring formation of epoxy groups. The products were then diluted and washed with acetone, and the solution was filtered to remove salt. The acetone and non-reacted epichlorohydrin in the filtered resin solution were evaporated using a rotary evaporator at 120 °C under reduced pressure. Lignin-based epoxy resin and cellulose-based epoxy resins were prepared following the same extraction and synthesis procedure as described.

2.2.3 Curing of the epoxy monomers

Samples used for the physical testing were prepared by solvent casting and the amount of curing agent was adjusted according to the resin's epoxy equivalent weight (EEW) value. Epikure W was used as a curing agent, and the resins were then placed in an oven for curing. The cure profile was designed as follows: 80 °C for 1 hour followed by 121 °C for 1 hour and 177 °C for 2 hours. Five samples were prepared and the average value was reported.

2.3 Characterization techniques

2.3.1 Epoxy equivalent weight (EEW)

The epoxy content of the synthesized resin was determined according to ASTM D1652. 0.2 - 0.8 g of epoxy resin was placed in a 50 mL flask and dissolved in 10 - 15 mL of methylene chloride. Crystal violet at 0.1 % w/w (4,4',4''-methylidynetris-(N,N-dimethylaniline) in glacial acetic acid was used as the indicator. The solution was titrated with 0.1 N of hydrogen bromide in acetic acid. The hydrogen bromide solution was standardized by 0.4 g of potassium hydrogen phthalate each time before EEW determination.

2.3.2 Differential scanning calorimetry (DSC)

Curing behavior and glass transition temperature (T_g) of the bio-epoxy resins were evaluated with a differential scanning calorimeter (DSC) model Q 100 from TA instruments under nitrogen atmosphere. Dynamic DSC measurements were carried out at a ramp rate of 5, 10, 15, and 20 °C /min at a temperature range from 30 to 300 °C to obtain the curing heat-flow curves of the liquid samples. Isothermal measurements were carried out from 140 - 170 °C. After, the cured samples were heated up to 300 °C at 10 °C /min to obtain the T_g of the fully cured samples.

2.3.3 Fourier transform infrared spectroscopy (FTIR)

FTIR analysis was performed on a Bruker Tensor 27 spectrometer with temperature controller - 10977. Samples were sandwiched between two KBr pellets. All FTIR spectra were recorded over 4000-400 cm⁻¹ wavenumbers at a resolution of 4 cm⁻¹ with 28 scans.

2.3.4 Thermogravimetric analysis (TGA)

Thermogravimetric analysis was performed using a TGA 2950 from 25 °C to 800 °C at a heating rate of 10 °C /min under air and nitrogen flow.

2.3.5 Gel permeation chromatography (GPC)

Gel permeation chromatography (GPC) analysis was conducted on a Waters 2695 separation module with a Waters 2998 photodiode array, a Waters 2414 refractive index detector, and two Waters Styragel 5 µm, HR 4E 7.8 × 300 mm column in series. The mobile phase used was HPLC grade THF, at 1.2 mL/min flow rate. The calibration curve was generated by narrow disperse

polystyrene standard from 156,000 Da to 580 Da in THF.

2.3.6 Nuclear magnetic resonance (NMR)

NMR spectra were obtained from a Varian NMR System 500 MHz spectrometer using a 5-mm carbon detection probe. 50 mg of samples were dissolved in deuterated solvents in the presence of 0.05% sodium 3-trimethylsilylpropionate-d₄ (TMSP) as an internal reference. Heavy water (D₂O) was chosen to dissolve bark extractives and deuterated chloroform (CDCl₃) was used to dissolve the rest of the epoxidized samples. All spectra were referenced to the ¹H and ¹³C signals of TMSP at 0 ppm. The ¹H spectrum was recorded at 25 °C after 526 scans. A 30° pulse flipping angle, a 3.98s acquisition time, and 1s relaxation delay time were used. The ¹³C NMR-1D NMR spectra were recorded at 25 °C after 1000 scans. A 30° pulse flipping angle, a 1.67s acquisition time, and 2s relaxation delay time were used.

2.3.7 Mechanical Universal Testing Machine

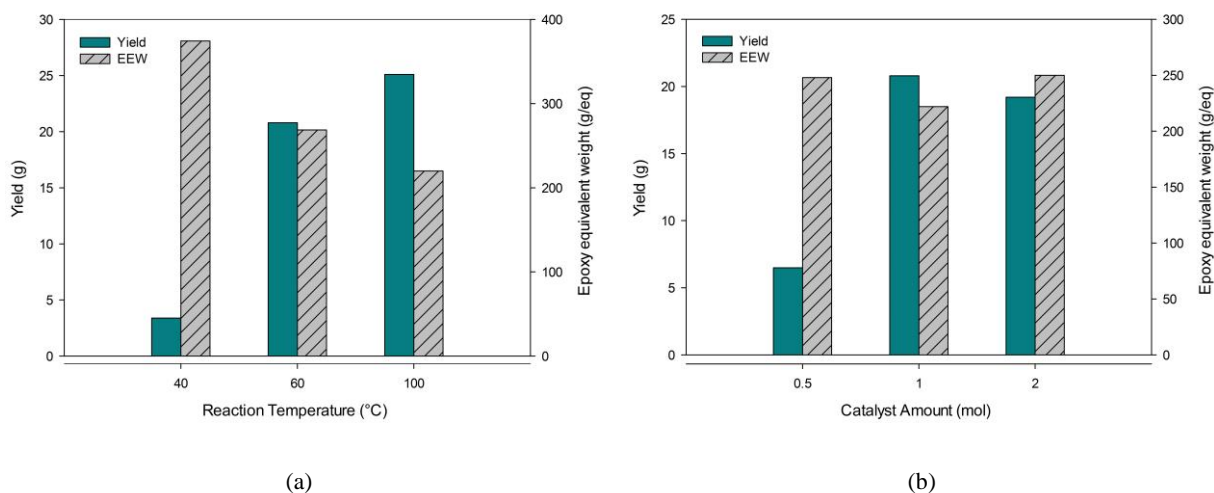
Tensile properties of the cured epoxy resins were tested at room temperature using ASTM type E tensile specimens. A standard computerized testing machine (Instron Model 20) was used in accordance with the ASTM D-638 procedure with a load cell of 2 kN and a cross head speed of 2.5 mm/min. Five specimens were measured for each formulation and analyzed using one-way ANOVA.

3. Results and discussions

3.1 Yield and epoxy equivalent weight (EEW)

The efficiency of the addition reaction of the epoxy group was significantly influenced by the reaction temperature and the amount of catalyst. Fig. 1 (a) shows the relationship between the yield and the reaction temperature for the extractive-based epoxy (E-Epoxy) synthesis. When the synthesis temperature increased, the yield of bio-resins also increased. However, higher temperatures resulted in more side reactions, which led to difficulties during the subsequent washing steps. In the solvent washing steps, acetone was first utilized to dissolve the crude products and remove the by-product, salt. To complete the purification and remove the remaining unreacted extractives, chloroform and water were then used for the liquid-liquid extraction. When the reaction temperature was above 80 °C, the emulsion layer of liquid-liquid extraction became thicker and remained longer due to the higher number of hydrolyzed epoxy rings. We also found that the EEW values reduced as the heating temperature increased, likely due to a higher substitution epoxidation.

The relationship between the yield and the catalyst amount is shown in Fig. 1 (b). When the catalyst molar ratio was equal to half of a mole, the epoxidation reaction proceeded minimally. In contrast, when the catalyst molar ratio was equal to two moles, the resins exhibited higher yield values possibly due to hydrolysis reactions during the synthesis. Our results indicated that the more suitable catalyst amount is 1 mole. Thus, in this study, the synthesis temperature was set at 60 °C, the catalyst amount at 1 mole, and the reaction time for 6 hours.



(Under 6 hours reaction time with 1 mol catalyst amount)

(Under 6 hours reaction time at 60 °C reaction temperature)

Fig. 1 Effect of reaction temperature (a) and catalyst amount (b) on the product yield and EEW value

3.2 Characterization of bio-epoxy resins

Fig. 2 (a) shows the IR spectra of the bark extractives, the E-Epoxy and the commercial epoxy resin (P-Epoxy). The characteristic absorption bands of bark extractives appear at 3417 cm⁻¹ (OH stretching), 2929 cm⁻¹ (CH₂ asymmetric), 2858 cm⁻¹ (CH₂ symmetric), 2715 cm⁻¹ (Aldehyde C-H), 1600 cm⁻¹ / 1426 cm⁻¹ (C=C aromatic rings), 1097 cm⁻¹ (C-O stretch in hemicellulose), and 1017 cm⁻¹

(C-H stretch in cellulose)²⁷. After the bark extractives were reacted with epichlorohydrin to form E-Epoxy, epoxy functionalization was confirmed by the observation of the absorption peak at 908 cm⁻¹ (asymmetric) and 852 cm⁻¹ (symmetric), corresponding to the vibration of the epoxide functional group²⁸⁻²⁹. Compared to the bark extractives, another significant difference was the lower OH stretching band intensity of E-Epoxy. Other characteristic peaks of E-Epoxy include aromatic C-H stretch (3055 cm⁻¹), aldehyde carbonyl stretch (1724 cm⁻¹), epoxy ring stretch (1252 cm⁻¹), and C-O-C stretch (1101 cm⁻¹). In addition, E-Epoxy contained a higher percentage of alkanes and carbonyl groups than P-Epoxy, which could be attributed to the presence of lignin and polysaccharide in the bark extractives.

To understand better the influence by the major components in the bark extractives, the IR spectra of epoxidized lignin extractives (L-Epoxy) and epoxidized cellulose extractives (C-Epoxy) are shown in Fig. 2 (b). L-Epoxy showed strong aromatic stretch absorption bands at 3052 cm⁻¹ (C-H stretch), 2263 cm⁻¹ / 2033 cm⁻¹ (Ring substitution pattern), and 1632 cm⁻¹ / 1501 cm⁻¹ (Ring stretch). In contrast, C-Epoxy had a long-chain band absorption at 710 cm⁻¹ and a strong alcohol vibration at 1113 cm⁻¹ which also appeared on the E-Epoxy IR spectrum.

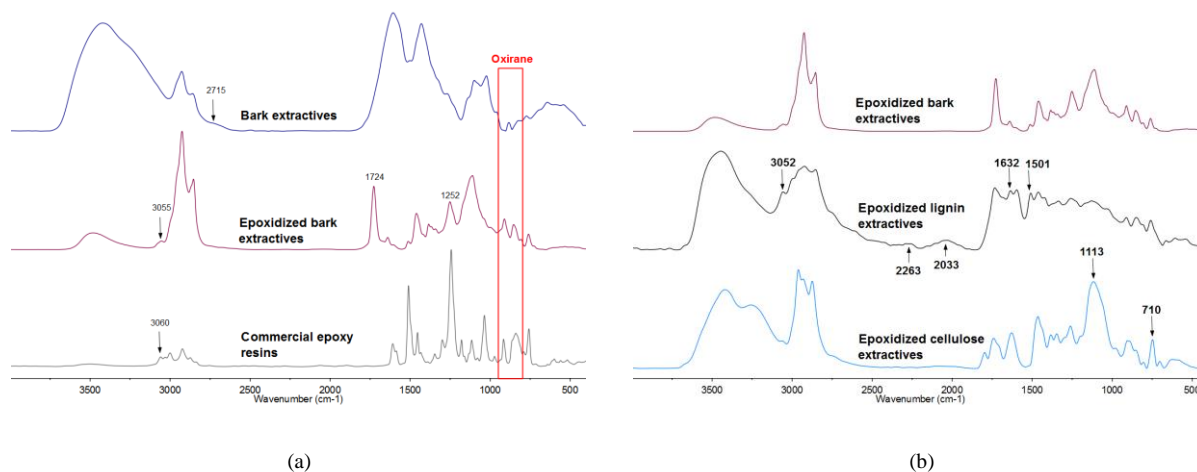


Fig. 2 FTIR spectra of (a) bark extractives, epoxidized bark extractives and commercial epoxy resin, (b) bio-epoxy resins

Successful functionalization of the bark extractives was also supported through ¹H NMR and ¹³C NMR spectroscopy. Epoxidized bark extractives (Fig. 3) showed fewer OH hydrogens from shifts at 3.6 ppm to 3.9 ppm and showed the appearance of signals at chemical shifts of 2.58, 2.77, and 3.13 ppm representing the epoxy rings and 3.3 and 3.6 ppm from the protons attached to an ether bond, differing from the bark extractives (Fig. 4). The chemical shifts at 9.8 ppm and 9.7 ppm were attributed to the protons attached on the aldehyde groups. Other aromatic ring protons are shown at 6.3 - 7.8 ppm, with the signal at 6.8 ppm particularly assigned to the aromatic protons in the guaiacyl unit³⁰.

The difficulty of analyzing the extractive-based epoxy resins by ¹H NMR was mainly caused by overlapping signals; therefore, the ¹³C NMR was used for further investigation. In the ¹³C NMR spectra, the aromatic structures from extractives and lignin were observed between 174.3 and 106.6 ppm as shown in Fig. 3 (b). The chemical shift at 174.3 ppm belongs to the carbonyl group on the linkage between catechin and gallic acid of the extractives³¹. The chemical shifts at 150.2 - 147.4 ppm, represent C₅ and C₇ attached with phenolic hydroxyl groups on the A ring, while chemical shifts at 146.7 - 144.6 ppm represent C_{4'} and C_{5'} attached with phenolic hydroxyl groups on the B ring. Other aromatic carbons in flavonoids structures show their chemical shifts at 130 ppm for the C_{1'}, at 115 - 110 ppm for C₈ (interflavonoid bond C₄ - C₈) and at 105 ppm for the C₆ (interflavonoid bond C₄ - C₆)³². The absence of the C₄ - C₆ interflavonoid band at 95 ppm and the presence of the C₄ - C₈ interflavonoid band at 105 ppm suggested that the units are exclusively linked to C₄-C₈, a classical pattern for a procyanidin. When C₄ connects with ring A, its chemical shift would be observed at 36.5 ppm and when C₄ is free, its chemical shift would be located at 29 ppm³³.

In addition, lignin fragments were observed in both the aromatic region (150-110 ppm) and the aliphatic region (72-54 ppm). These peaks were also confirmed by comparing with the lignin-based epoxy resin (Fig. 5). The major mono-lignin unit in pine bark is guaiacyl (G) and the dilignin that commonly contains beta-O-4 bonding (48%) and biphenyl bonding (9.5-11%)³⁴. The chemical shifts at 150-145 ppm were assigned to the C₃ and C₄ on the G unit. The chemical shifts at 134 ppm, 132 ppm, and 126 ppm correspond to C₁, C₅ (etherified), and C₅ (non-etherified), respectively. Other aromatic carbons in the lignin fraction include chemical shifts at 123 ppm (C₁ and C₆ in ϕ -C(=O)C-C units), 113 ppm (C₅ in G units), and 110 ppm (C₂ in G units). In the aliphatic region, C _{α} (71.8 and 71.2 ppm), C _{β} (129 and 54 ppm), and C _{γ} (63 and 62 ppm) were also observed³⁰.

Furthermore, the chemical shifts at 44.1 ppm, 50.7 ppm, and 69.3 ppm are related to the epoxy rings. Note that the absence of chemical shift at 45.2 ppm implies that there is undetectable level of residual or unreacted level of epichlorohydrin in our bio-resins. Therefore, the liquid-state NMR confirmed that the bark extractives were successfully epoxidized with epichlorohydrin and that by NMR the backbone structures are more similar to lignin than to cellulose (Fig. 6).

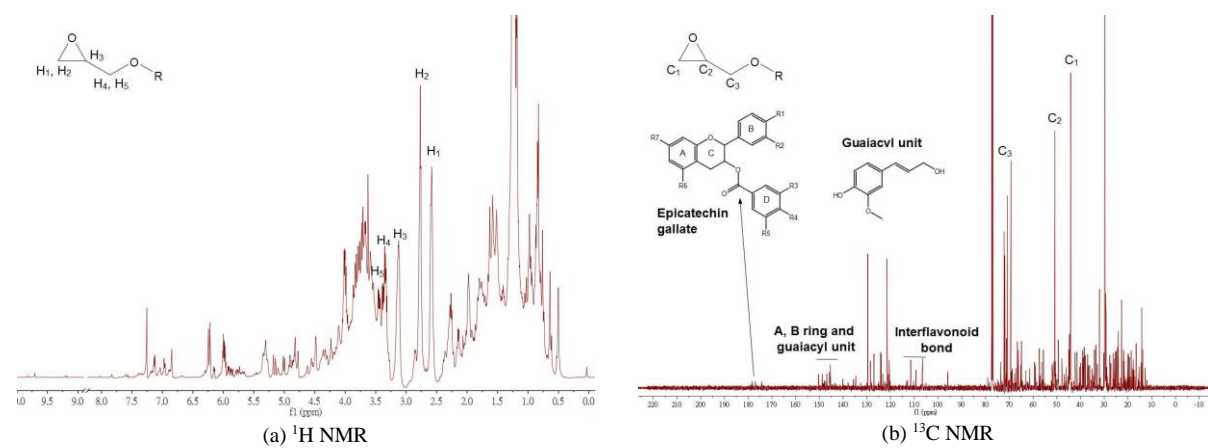


Fig. 3 Liquid state NMR spectrum of the extractive-based epoxy monomers

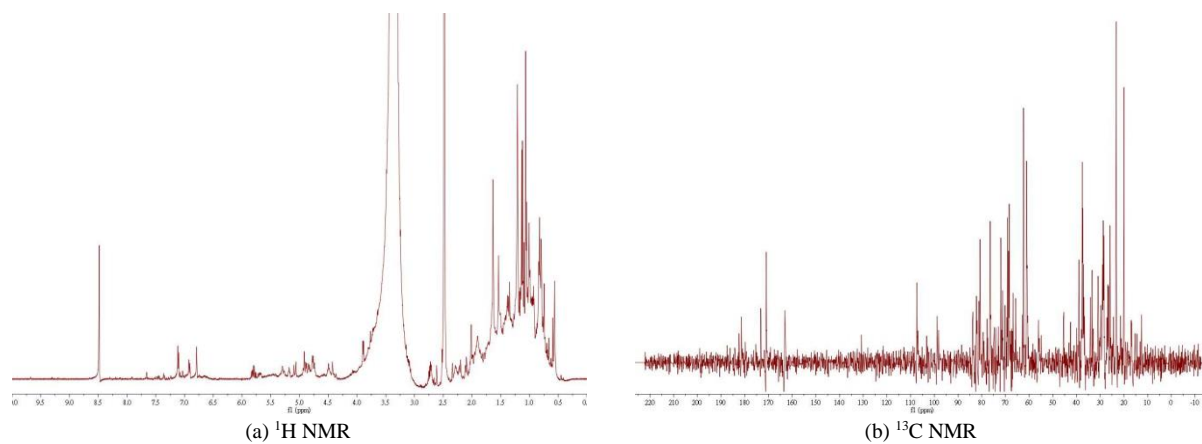


Fig. 4 Liquid state NMR spectrum of the bark extracts

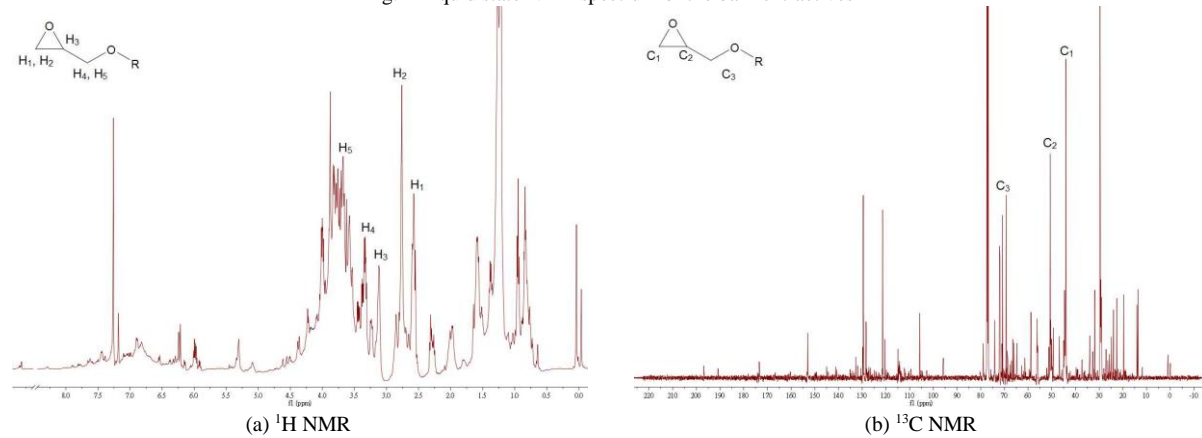


Fig. 5 Liquid state NMR spectrum of the lignin-based epoxy monomers

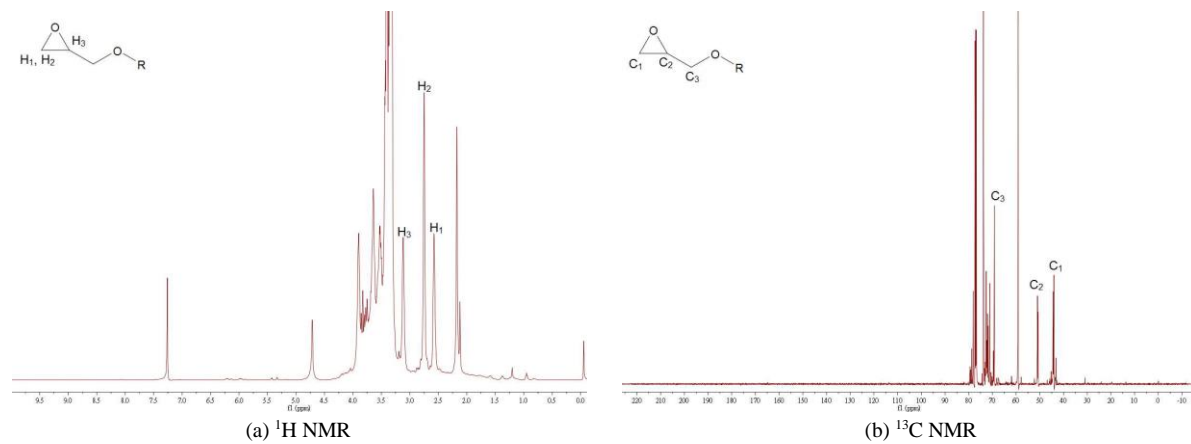


Fig. 6 Liquid state NMR spectrum of the cellulose-based epoxy monomers

GPC was used to evaluate the molecular weights of the E-Epoxy and L-Epoxy. In Table 1, the number average molecular weight (M_n) of E-Epoxy is shown to be 588 Da and the polydispersity to be 1.36, while that of L-Epoxy are 1071 Da and 2.06, respectively. Compared to L-Epoxy, E-Epoxy exhibited a lower molecular weight and narrower polydispersity, which may offer more uniform performance of the cured resin.

Origin software (version 8.6; Microcal Software Inc., Northampton, MA) was used to separate the multi-peaks in the GPC results. Three peaks were identified in E-Epoxy and four peaks were identified in L-Epoxy. Comparing Fig. 7 (a) with (b), the first peak of L-Epoxy is 3891 Da, which is similar to the molecular weight reported for alkali lignin by other researchers^{26, 35}. We suggest that the first peak of E-Epoxy (1071 Da) and the second peak of L-Epoxy (1396 Da) are from epoxidized lignin fragments with 5 or 6 monolignol monomers. The second peak of E-Epoxy (513 Da) may be an epoxidized catechin which reacted with four epichlorohydrin units. This is a likely explanation since the peak of 528 – 529 Da is the most common repeating unit shown in commercial tannins³¹. The third peak (345 Da/372 Da) and fourth peak (277 Da) might be assigned to the epoxidized resin acid and epoxidized coniferyl alcohol, respectively.

Table 1 Molecular weight and polydispersity of E-Epoxy and L-Epoxy

	M_n	M_w	PDI	Peak1	Peak2	Peak3	Peak4
E-Epoxy	588 (26)	796(21)	1.36	1071	513	345	-
L-Epoxy	1071(43)	2210(39)	2.06	3891	1396	372	277

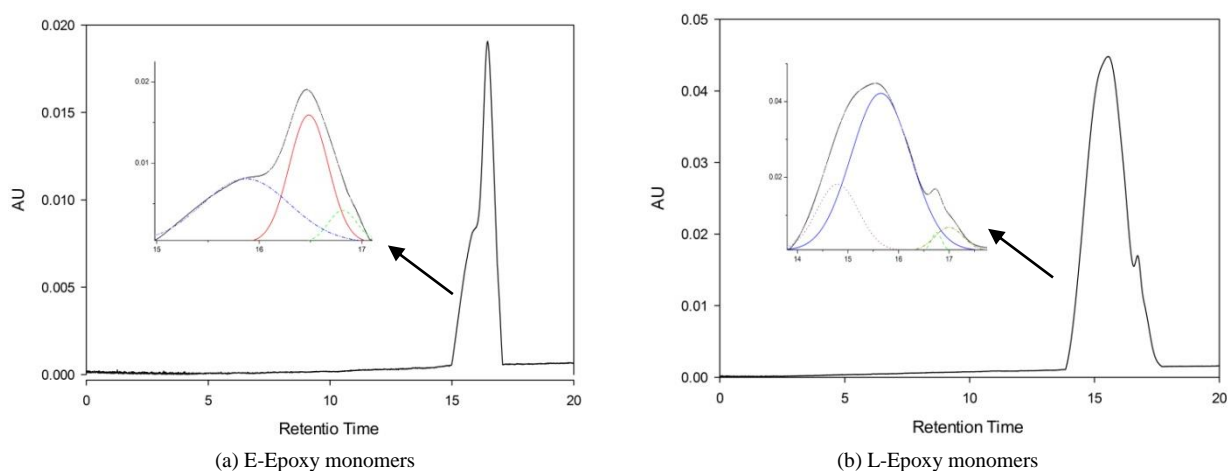


Fig. 7 GPC traces of uncured bio-epoxy resins

3.3 Curing behavior

DSC is a useful technique for studying cross-linking reactions of thermosetting epoxy resins. Non-isothermal DSC analysis was chosen in this study to avoid diffusion control, which can affect the calculation of kinetic parameters. As in many thermosetting polymers, diffusion and vitrification also occur in epoxy systems. Performing the analysis with a constant heating rate can improve segment mobility, which lessens the effect of these phenomena. The raw DSC plots are shown in supplementary materials.

Among the various multiple heating rate methods, the Kissinger equation is the most extensively used method to calculate the activation energy, which is expressed as:

$$\ln(\beta/T_p^2) = \ln(A \times R/E_a) - (E_a/RT_p) \quad \text{Eq. (1)}$$

where, β is the heating rate, T_p is the temperature at which the maximum heat flow rate occurs, A is the pre-exponential factor (Arrhenius factor), R is the gas constant, and E_a is the activation energy.

Using the Kissinger equation, E_a for commercial resin was 52.0 kJ/mol and E_a for the bio-resins was 42.0 kJ/mol, both of which fall in the typical range of E_a for common epoxy-amine polymerization systems (40–70 kJ/mol). The extractive-based resins have a lower activation energy and a higher reactivity compared to the commercial products, possibly due to the abundant hydroxyl groups in the bark components enhancing the autocatalytic reactions in the bio-epoxy system.

However, one of the limitations of the Kissinger equation is that the reaction mechanism is assumed to be n^{th} order. Considering that the real E_a value varies with the conversion rate, the Kissinger-Akahira-Sunose's (KAS) isoconversional equation was applied to observe the evolution of E_a with the conversion rate. The basic assumption of this analysis is that the reaction rate at a constant conversion depends only on temperature. In kinetic analysis, it is generally assumed that the rate of reaction can be described by two functions $k(T)$ and $f(\alpha)$,

$$d\alpha/dt = k(T)f(\alpha) = A \exp(-E_a/RT)f(\alpha) \quad \text{Eq. (2)}$$

where, $k(T)$ is the rate constant, and $f(\alpha)$ is the reaction model. When the heating rate is constant, equation (2) can be rewritten as

$$d\alpha/dT = A \exp(-E_a/RT)f(\alpha)/\beta \quad \text{Eq. (3)}$$

As shown in equation (3), isoconversional methods offer an assumption-free estimation of the activation energy. The fundamental assumption of the isoconversional model is that the reaction rate is only a function of temperature:

$$(d \ln/dT)(d\alpha/dt)_\alpha = E_{a,\alpha}/R \quad \text{Eq. (4)}$$

where $E_{a,\alpha}$ is the activation energy at a given conversion. Note that the KAS method offers a significant improvement in the accuracy of the E_a value compared to the Ozawa–Flynn–Wall method³⁶.

Fig. 8 shows the values for E_a at different curing conversions, α , determined by the KAS method for non-isothermal data. It is worth noting that the E_a of commercial resins varies within a narrow range of 3.4 kJ/mol with respect to α . So the constant E_a values implied the diffusion control resulted in negligible influence on the non-isothermal data of the test samples. Compared to commercial products, bio-epoxy resins have a higher activation energy before 30 % conversion and a lower activation energy after 30 % conversion. The following two reasons may account for this observation: First, the molecular weight of bio-resins is higher than that of the commercial product that can result in a lower mobility of the molecular chain movement and a higher activation energy at the initial stage. Second, the viscosity of the reaction mixture decreases dramatically with increasing temperature, which helps to promote the reaction at its final stage³⁷⁻³⁸. This non-constant activation energy trend indicates that the non-isothermal reaction of bio-resins/amine curing agent probably follows a multi-step mechanism³⁸.

In addition, an important aim of the curing study was to predict the curing behavior of the bio-epoxy resins. After obtaining the values for the kinetic parameters by the KSA method, we plotted the predicted rate curve for isothermal data, as shown in Fig. 9. Compare to the ASTM E698 method, several studies have indicated that the Vyazovkin method is more precise and suitable for epoxy-amine curing kinetics prediction³⁹⁻⁴⁰. The Vyazovkin method uses the following equations³⁶:

$$g(\alpha) = t_\alpha A_\alpha \exp(-E_a/RT_0) \quad \text{Eq. (5)}$$

$$g(\alpha) = (A_\alpha / \beta) \int_{T_0}^{T_\alpha} \exp(-E_a/RT) dT \quad \text{Eq. (6)}$$

Equations (5) and (6) stand for the isothermal cure at $T_c = T_0$ and non-isothermal cure at heating rate β , respectively. To obtain t_α , equation (6) can be divided by equation (5):

$$t_\alpha = \left[\int_{T_0}^{T_\alpha} \exp(-E_a/RT) dT \right] / \beta \exp(-E_a/RT_0) \quad \text{Eq. (7)}$$

Equation (7) enables the determination of time for a given conversion. Fig. 9 shows the isothermal epoxy cure from 140 to 170 °C as predicted by using the E_a dependence derived earlier. The overall model prediction gave satisfactory agreement with the experimental isothermal measurements and only at high conversion rates (> 50 %), where the predicted curing time is slightly lower than the experimentally determined reaction time. The same observation was reported by other groups^{39, 41}.

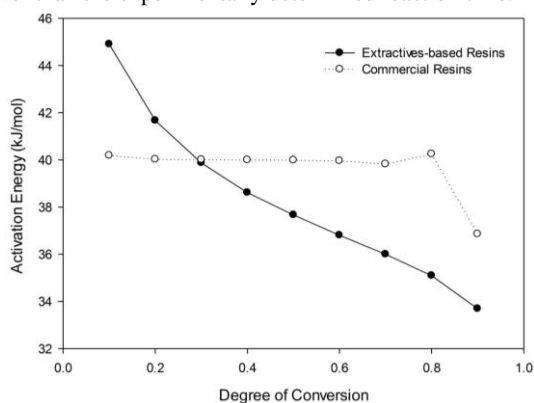


Fig. 8 Dependence of the activation energy on the extent of conversion evaluated from non-isothermal DSC data

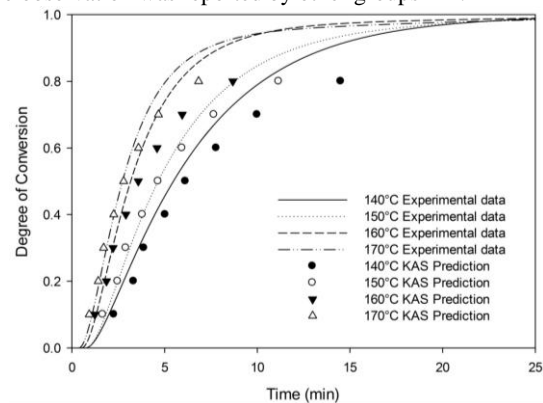


Fig. 9 Model-free prediction of isothermal cure from 140 to 170 °C using KAS method (The experimental data are shown by line. The points correspond to the predicted time)

Furthermore, FTIR was used to monitor the concentration of epoxy functional groups during the formation of networks, as shown in Fig. 10. The spectra were normalized to a reference absorption at 1184 cm^{-1} that represents the C–C stretch of bisphenol⁴². The signal reduction at 908 cm^{-1} as well as at 880 cm^{-1} displayed the consumption of epoxy groups, whereas the signal increase at 940 cm^{-1} revealed the formation of a new bond.

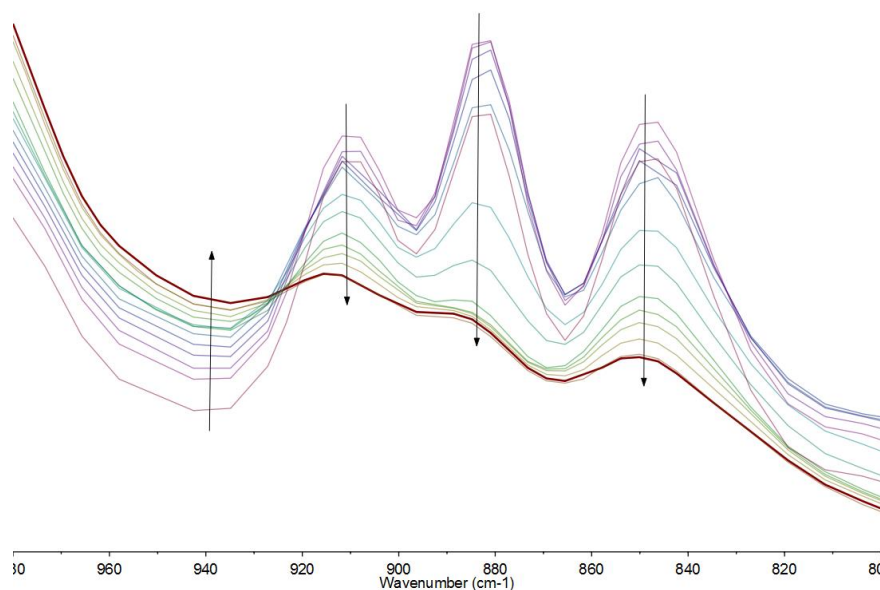


Fig. 10 Evolution of oxirane functional group during curing

3.4 Mechanical performance

Bio-epoxy resins were blended with commercial epoxy resins (at 10 %, 30 %, and 50 % w/w of bio-epoxy) and then cured with the hardener EPIKURE W at 80 °C for 1 hour, 121 °C for 1 hour and 177 °C for 2 hours. The hardener EPIKURE W is an aromatic-type curing agent, providing samples with low viscosity and high strength. Fig. 11 shows the tensile properties of the cured 10 %, 30 %, and 50 % bio-epoxy resins, which display comparable properties to commercial products. Based on one-way ANOVA, there is no significant difference in the tensile strengths among the four groups ($p=0.087$).

Bark-derived epoxy resins have a higher tensile strength (63 MPa) than liquefied wood-based epoxy (58MPa)⁴³ and epoxidized soybean oil-based epoxy (29MPa)⁴⁴. The high stiffness of the bark-based epoxy resin is an attractive property as an alternative product. Compared to the long chain structure of epoxidized soybean oil, bark-based or liquefied wood-based epoxy has higher potential to be applied in the automobile or aerospace industries. The lower tensile modulus might be attributed to the bulky ring structures in extractives, which decreases the crosslink density of the system⁴⁵.

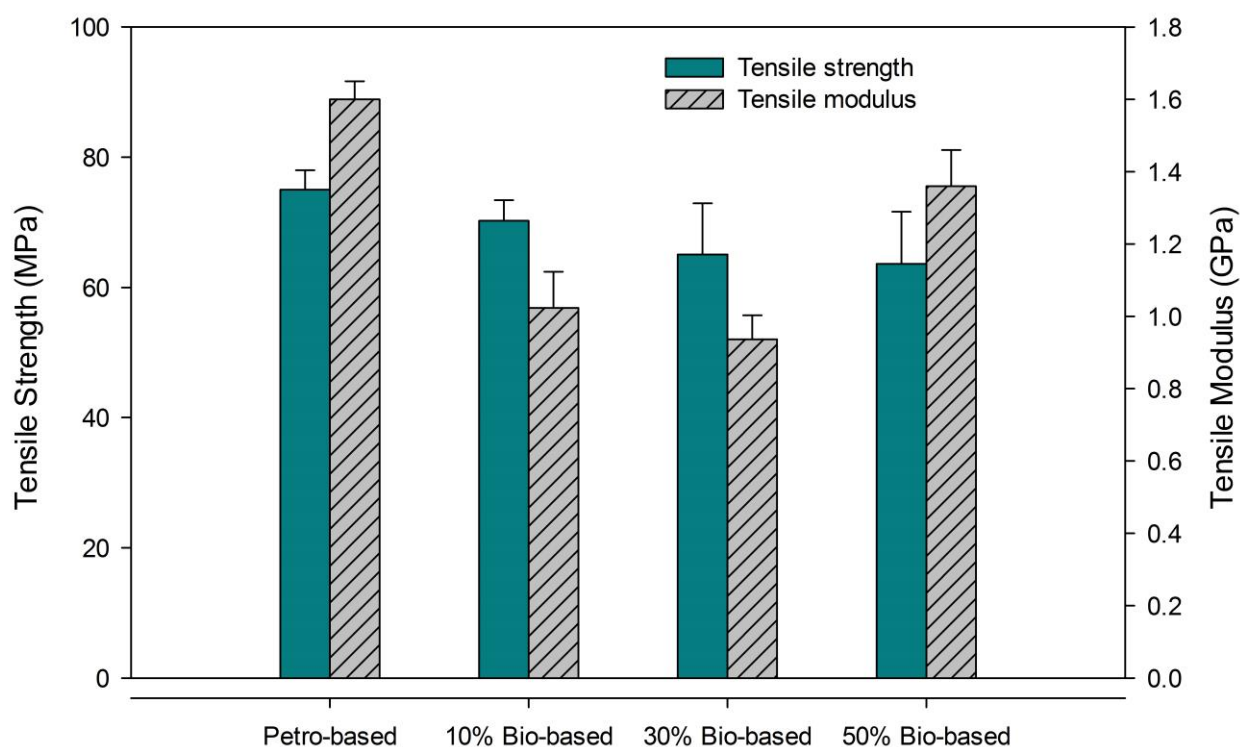


Fig. 11 Tensile strength and modulus of the cured epoxy resins

3.5 Thermal degradation and thermal stability

TGA is used to evaluate thermal oxidation and thermal stability of the polymers. The experiments were conducted under air and inert gas, respectively. Fig. 12 displays the TGA plots obtained from testing commercial epoxy resins and bio-epoxy resins in air, while Fig. 13 shows the results of TGA tests under a nitrogen atmosphere.

The commercial product has a strong degradation peak for thermal oxidation at about 382°C. The bio-epoxy resins exhibited similar thermal degradation patterns. But bio-epoxy also shows the presence of new peaks at temperatures of 310°C and 345 °C, which can be caused by phase separation occurring in the network. The combustion process can be divided into three stages: between 300-340 °C, 340-390 °C, and 480-600 °C. For the commercial samples and 10 % and 30 % bio-epoxy samples, the first stage showed a mass loss of 0.8-0.9 %, the second stage showed 64-67 % mass loss and the last stage showed a mass loss of 32-35 %. However, for the 50 % bio-epoxy samples, the mass loss at the first stage increased to 17 % and at the second stage decreased to 41 %, suggesting that more thermally sensitive compounds exist in the bio-epoxy resins. Some other bio-based epoxy resins also displayed their degradation temperatures at around 274-305 °C.⁷

To understand the thermal stability of the novel epoxy resins, the commercial product and extractive-based and lignin-based epoxy resins were heated in a nitrogen atmosphere, the results of which are shown in Fig. 13. The black lines represents the weight loss of the cured resins. Compared to the petro-based epoxy, the weight loss of bio-based epoxy was faster between 250 to 400°C. The weight loss curves were transformed into their first derivative (green lines), which indicates the points of highest rate of change in the weight loss. The commercial epoxies only showed one degradation peak at 392°C, which corresponds to the HCN bond breaking⁴⁶. In comparison, the extractive-based epoxy exhibited two degradation peaks. The first peak is at 349 °C, which is same to the shoulder shown in the curve for the lignin-based epoxy resin, and the second peak was presented at 392°C, which is same to the degradation peak of HCN bonding. In addition, the statistic heat-resistant index temperature (T_s) is given in Table 2. This value was determined from the temperatures at 5 % weight loss (T_{d5}) and 30 % weight loss (T_{d30}) of the sample obtained by TGA, following Eq. (5):

$$T_s = 0.49(T_{d5} + 0.6(T_{d30} - T_{d5})) \quad \text{Eq. (5)}$$

The values of the statistic heat-resistance of the extractive-based epoxy resins were similar to the lignin-based epoxy resin but lower compared to the commercial product. Several studies reported that bio-based resins exhibited lower thermal degradation temperature compared to that of the petroleum resins⁴⁵. Compared to other bio-epoxy resins, however, extractive-based epoxy resins showed comparable performance. Therefore, additional refining steps, such as extraction of unreacted monomers, might be

beneficial to further improve thermal properties of the extractive-based epoxy resins.

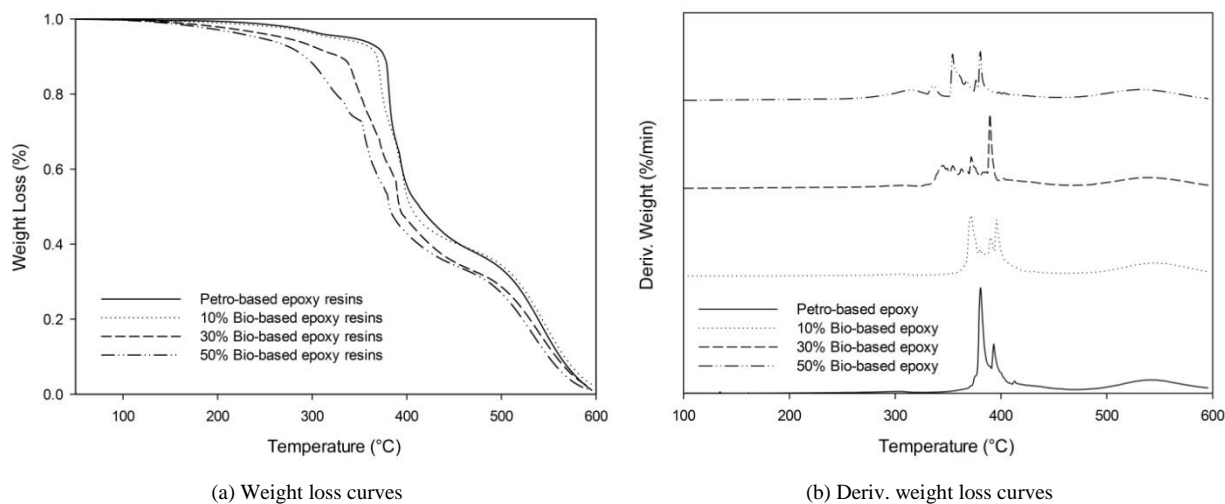


Fig. 12 Thermal degradation of the cured epoxy resins under air

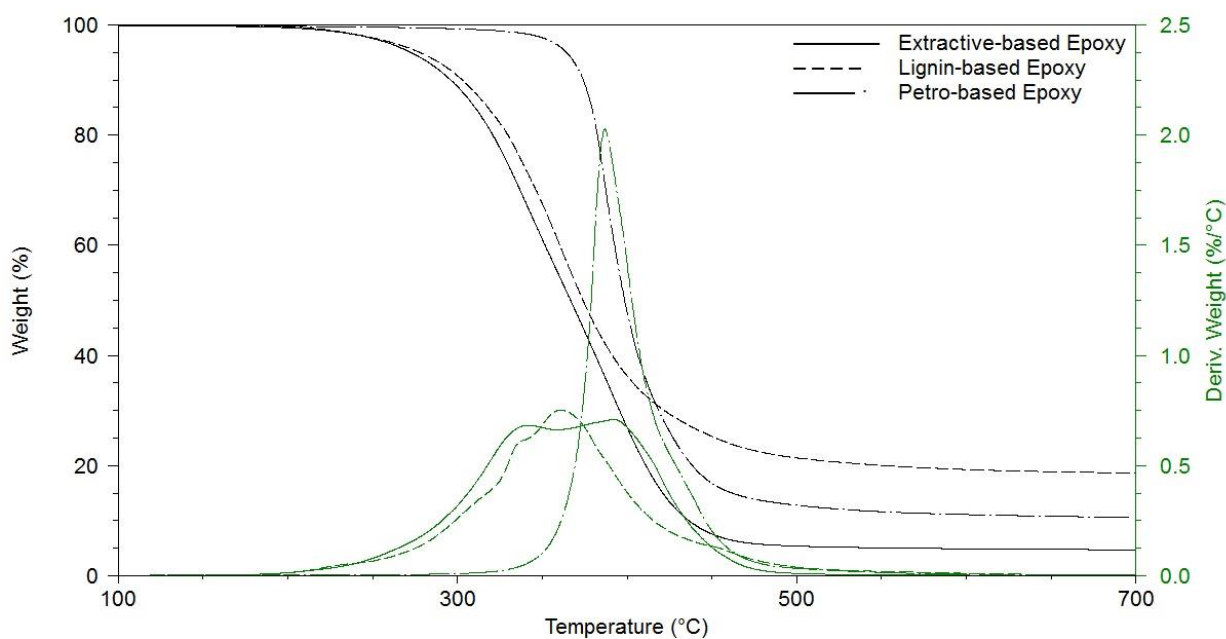


Fig. 13 Thermal stability of the cured epoxy resins under nitrogen atmosphere

Table 2 TGA data of the cured epoxy resins

	$T_{d\ onset}$ (°C)	T_{d5} (°C)	T_{d30} (°C)	T_s (°C)	Char ₇₀₀ (%)
100 % Petro-based epoxy	369	353	383	182	12.2
100% Extractive-based epoxy	294	272	337	152	4.6
100% Lignin-based epoxy	297	277	346	156	18.1

4. Conclusions

This study examined the feasibility of using bark extractives to formulate bio-epoxy resins. FTIR, NMR, and GPC methods were applied to identify the chemical structures and molecular weights of the epoxies synthesized in this study. For uncured bio-epoxy

monomers, the absorption of epoxy groups was observed at 908 cm⁻¹ in the FTIR spectrum and the same groups were seen at 45 and 51 ppm in the ¹³C-NMR spectrum. Both analyses indicated successful glycidylation of bark extractives after reaction with epichlorohydrin. Furthermore, the GPC results showed that bark extractive-based epoxy resins have a lower molecular weight (588 Da) compared to the lignin-based epoxy resins (1071 Da). Based on the Kissinger kinetic analysis, the activation energy of the extractive-based epoxy resin is lower than that of the commercial products due to the abundant hydroxyl groups in extractive promoting the autocatalytic network formation. The curing time of the bio-epoxy resin was successfully predicted using non-isothermal data analyzed by the KAS method.

For the cured epoxy resins, mechanical performance and thermal properties showed that the novel synthesized bio-epoxy resins displayed mostly comparable properties as the commercial product. Therefore, bark extractives have great promises to be used as the raw material to synthesize epoxy resins replacing toxic bisphenol A.

Acknowledgments

The authors would like to thank ORF-RE (Bark Biorefinery) and NSERC-Strategic Network Plastic Manufacturing partners for the financial support and Dr. Tjong from Ford Motor Company for the technical support and guidance. Appreciation is extended to Nicolas Tanguy, Lynn Wei and Lindsey Fiddes for their generous help and support. Finally, we also like to thank Momentive Inc. for providing the commercial resin samples.

References

1. A. E. Gerbase, C. L. Petzhold and A. P. O. Costa, *J Am Oil Chem Soc*, 2002, **79**, 797-802.
2. H. Miyagawa, A. K. Mohanty, R. Burgueno, L. T. Drzal and M. Misra, *J Polym Sci Pol Phys*, 2007, **45**, 698-704.
3. A. Overeem, G. J. H. Buisman, J. T. P. Derksen, F. P. Cuperus, L. Molhoek, W. Grisnich and C. Goemans, *Ind Crop Prod*, 1999, **10**, 157-165.
4. S. Hirose, *J Oil Palm Res*, 2011, **23**, 1110-1114.
5. T. R. Cuadrado and R. J. J. Williams, *Polym Commun*, 1989, **30**, 239-240.
6. T. W. Abraham and R. Hofer, in *Polymer science: A comprehensive reference*, ed. M. M. K. Matyjaszewski, Elsevier, Oxford, 2012, vol. 10, ch. 3, pp. 15-58.
7. D. Fourcade, B. S. Ritter, P. Walter, R. Schonfeld and R. Mulhaupt, *Green Chem*, 2013, **15**, 910-918.
8. Y. Hasegawa, K. Shikinaka, Y. Katayama, S. Kajita, E. Masai, M. Nakamura, Y. Otsuka, S. Ohara and K. Shigehara, *Sen-I Gakkaishi*, 2009, **65**, 359-362.
9. C. Sasaki, M. Wanaka, H. Takagi, S. Tamura, C. Asada and Y. Nakamura, *Ind Crop Prod*, 2013, **43**, 757-761.
10. Q. Q. Ma, X. Q. Liu, R. Y. Zhang, J. Zhu and Y. H. Jiang, *Green Chem*, 2013, **15**, 1300-1310.
11. H. Kishi and A. Fujita, *Environ Eng Manag J*, 2008, **7**, 517-523.
12. H. Kishi, A. Fujita, H. Miyazaki, S. Matsuda and A. Murakami, *J Appl Polym Sci*, 2006, **102**, 2285-2292.
13. H. Pan, *Renew Sust Energy Rev*, 2011, **15**, 3454-3463.
14. S. G. Tan and W. S. Chow, *J Am Oil Chem Soc*, 2011, **88**, 915-923.
15. J. M. Raquez, M. Deleglise, M. F. Lacrampe and P. Krawczak, *Prog Polym Sci*, 2010, **35**, 487-509.
16. T. Koike, *Polym Eng Sci*, 2012, **52**, 701-717.
17. S. N. Cheng, I. D'cruz, M. C. Wang, M. Leitch and C. B. Xu, *Energy Fuel*, 2010, **24**, 4659-4667.
18. E. Windeisen and G. Wegener, in *Polymer science: A Comprehensive Reference*, ed. M. M. K. Matyjaszewski, Elsevier, Oxford, 2012, vol. 10, ch. 15, pp. 255-266.
19. J. O. Wegner, ed. R. Höfer, Royal Society of Chemistry, Cambridge, 2009, ch. 11, pp. 425-435.
20. G. K. Gupta, Master Thesis, University of Toronto, 2009.
21. D. G. Briggs, University of Washington Institute of Forest Resources, Seattle, 1994, ch. 9, pp. 106-110.
22. M. H. Alma and S. S. Kelley, *Polym Degrad Stabil*, 2000, **68**, 413-418.
23. Y. Zhao, N. Yan and M. Feng, *Int J Adhes Adhes*, 2010, **30**, 689-695.
24. J. D'Souza and N. Yan, *Acs Sustain Chem Eng*, 2013, **1**, 534-540.
25. E. Aspe and K. Fernandez, *Ind Crop Prod*, 2011, **34**, 838-844.
26. B. Xiao, X. F. Sun and R. C. Sun, *Polym Degrad Stabil*, 2001, **74**, 307-319.
27. Y. Zhao, Ph.D. Thesis, University of Toronto, 2013.
28. S. Q. Ma, X. Q. Liu, Y. H. Jiang, Z. B. Tang, C. Z. Zhang and J. Zhu, *Green Chem*, 2013, **15**, 245-254.

29. D. L. Pavia, G. M. Lampman and G. S. Kriz, in *Introduction to Spectroscopy: A Guide for Students of Organic Chemistry*, Saunders (W.B.) Co Ltd, Philadelphia, 1979, ch. 2.
30. J. Z. Mao, L. M. Zhang and F. Xu, *Cell Chem Technol*, 2012, **46**, 193-205.
31. P. Navarrete, A. Pizzi, H. Pasch, K. Rode and L. Delmotte, *Ind Crop Prod*, 2010, **32**, 105-111.
32. I. Wawer, M. Wolniak and K. Paradowska, *Solid State Nuclear Magnetic Resonance*, 2006, **30**, 106-114.
33. K. Lorenz and C. M. Preston, *Journal of Environmental Quality*, 2002, **31**, 431-437.
34. E. Adler, *Wood Sci Technol*, 1977, **11**, 169-218.
35. S. Tsuda, K. Nakagawa, T. Oyama, A. Takahashi, Y. Okabe, H. Kagawa, S. Yamada and Y. Okabe, *J. Network Polym. Jpn.*, 2010, **31**, 701-717.
36. S. Vyazovkin, A. K. Burnham, J. M. Criado, L. A. Perez-Maqueda, C. Popescu and N. Sbirrazzuoli, *Thermochim Acta*, 2011, **520**, 1-19.
37. G. Vazquez, J. Gonzalez-Alvarez, F. Lopez-Suevos, S. Freire and G. Antorrena, *J Therm Anal Calorim*, 2002, **70**, 19-28.
38. S. Vyazovkin and N. Sbirrazzuoli, *Macromol Rapid Comm*, 2006, **27**, 1515-1532.
39. S. Vyazovkin and N. Sbirrazzuoli, *Macromolecules*, 1996, **29**, 1867-1873.
40. V. P. Privalko, V. Y. Kramarenko, V. L. Sokol and A. M. Karateev, *Polym Polym Compos*, 1998, **6**, 331-336.
41. L. Gan, Z. J. Sun, Y. Z. Gu, M. Li and Z. G. Zhang, *Acta Polym Sin*, 2010, **8**, 1016-1022.
42. D. W. Sohn and K. J. Ko, *Korea Polym J*, 1999, **7**, 181-188.
43. T. Asano, M. Kobayashi, B. Tomita and M. Kajiyama, *Holzforschung*, 2007, **61**, 14-18.
44. Z. S. Petrović, *Contemporary Materials*, 2010, **1**, 39-50.
45. X. Q. Liu, W. B. Xin and J. W. Zhang, *Green Chem*, 2009, **11**, 1018-1025.
46. J. Madarasz and G. Pokol, *J Therm Anal Calorim*, 2007, **88**, 329-336.

